2.2 USE OF AN ARTIFICIAL NEURAL NETWORK TO FORECAST THUNDERSTORM LOCATION

Waylon Collins* and Philippe Tissot**
*NOAA/National Weather Service
**Texas A&M University – Corpus Christi

1. INTRODUCTION

Deterministic Numerical Weather Prediction (NWP) models integrate the conservation equations of atmospheric mass, heat, motion, and water. With respect to *gridpoint* NWP models, the difference terms in the equations are approximated as taylor expansions and are integrated forward in time (Pielke 2002). Processes resolved on the grid-scale are referred to as *model dynamics*. Sub-grid scale processes in NWP models must be accounted for—otherwise the quality of the numerical predictions will rapidly degrade with time. These sub-grid scale processes—which by definition cannot be explicitly determined by the model—are parameterized in terms of the grid-scale. These parameterizations are referred to as *model physics* (Kalnay 2003). The parameterization important to this paper is convection - those processes related to shower and thunderstorm activity. The purpose of convective parameterization (CP) is to reduce atmospheric instability to prevent the model from generating excessive grid-scale precipitation. Precipitation is simply a by-product of the CP process. Thus, such convection is not explicitly predicted. However, if model grid-spacing is decreased to around 2-km (the mesoscale/microscale boundary), convection can be explicitly predicted thus rendering convective parameterization mute. However, such an increase in model resolution will require enormous computing resources (CyRDAS 2004) -- unrealistic for operational applications at present. Further, it is unclear whether increasing the horizontal resolution will improve forecast accuracy. Mass et. al (2002) suggest that increasing horizontal resolution of NWP models to 4-km may not provide additional accuracy. According to Fabry (2006), the exact location of convective cells that develop during the daytime is generally determined by the location of updrafts on the meso-γ (2-20 km) or smaller scales. According to Orlanski (1975), individual deep convective cells occur on the micro-α scale (200m-2km). However, based on 2-D deterministic numerical atmospheric simulations, Zeng and Pielke (1995) found that vertical velocities—induced by surface heterogeneity on flat terrain—are generally unpredictable on length scales less than 5-km.

The lead author proposes a paradigm shift away from the idea of increasing NWP model horizontal resolution to explicitly forecast the development of thunderstorms, hereafter referred to as convective initiation (CI). The method presented in this paper is an attempt to improve the forecast accuracy of CI, up to 24 hrs in advance, and within an accuracy of 400 km^2.

• Corresponding author address: Waylon G. Collins, National Weather Service, 300 Pinson Drive, Corpus Christi, TX 78406; e-mail: Waylon.Collins@noaa.gov

A feed-forward, supervised, multi-layer perceptron Artificial Neural Network (ANN) was developed to test the hypothesis that an ANN can be developed to successfully forecast CI, based on the following input categories. The first category consists of seventeen (17) output parameters from a hydrostatic mesoscale NWP model known as the Eta (e.g. Rogers et. al. 1996). The specific Eta input parameters chosen were based on their influence on CI/convective dissipation. Eta model integrations took place on a grid with a horizontal grid spacing of 12-km - within the meso-γ scale. However, subgrid scale atmospheric processes that directly contribute to CI cannot be accounted for explicitly by the Eta. A solution is to incorporate a second category of input data—subgrid scale data that directly influence CI. One such data type is Land Surface Temperature (LST) – at a grid spacing of 1-km (micro-α scale) - derived from the NASA Moderate Resolution Imaging Spectroradiometer (MODIS) instrument aboard the Terra and Aqua satellites. For additional information, see URL http://modis.gsfc.nasa.gov. Land surface heterogeneity (variations in soil moisture, vegetation, soil type, etc.) contributes to differential surface heating – which results in LST and air surface temperature gradients. These gradients contribute to microscale/meso-γ scale convergent wind patterns which in turn contribute to CI (e.g. Avissar and Liu 1996). Additional sub-grid scale data that influence CI are horizontal thermal gradients near the edges of persistent cloud cover (e.g. Markowski et. al. 1998). The MODIS parameter that measures the percentage of clear sky coverage also served as input into the ANN. The third type of subgrid scale data ingest is the Aerosol Optical Depth (AOD), which may influence cloud microphysics, thunderstorm dynamics, and the subsequent amount of lightning associated with thunderstorms.

Thus, in this approach the Eta output provides a forecast of whether the larger scale mesoscale environment is conducive to CI while the subgrid data determines the extent to which convection could be triggered at a particular location. This study will test the utility of using an ANN to incorporate numerical model and subgrid scale data to improve the forecasting of CI on both spatial and temporal scales.

2. ARTIFICIAL NEURAL NETWORKS

An Artificial Neural Network (ANN) is a computational model that is loosely based on the manner in which the human brain processes information. Specifically, it is a network of highly interconnecting processing elements (neurons) operating in parallel (Figure 1). An ANN can be used to solve problems involving complex relationships between variables. The particular type of ANN used in this study is a supervised one, wherein an output vector (target) is specified, and the ANN is trained to minimize the error between the

output and input vectors, thus resulting in an optimal solution. This is accomplished by adjusting the connections between the elements (the weights). In theory, this adjustment process can be viewed as a form of 'learning'. Thus, the ANN is considered to be a form of artificial intelligence (AI). ANNs were selected for this study in large part because of their ability to model non-linear relationships. The relationship between the input and output parameters in this study are highly non-linear. Additional information on Artificial Neural Networks can be found in references such as Beale (1990) and Hagan et al. (1996).

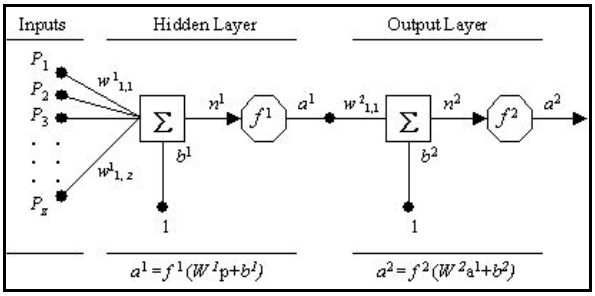

Figure 1: A 2-layer ANN with multiple inputs and single hidden and output neurons

3. METHODOLOGY

A grid of 14 x 23 equidistant points (20-km grid spacing) was developed which covers a region slightly larger than the County Warning and Forecast Area (CWFA) responsibility of the National Weather Service (NWS) forecasters in the Weather Forecast Office (WFO) in Corpus Christi Texas (CRP). These points create 286 square regions (hereafter referred to as 'boxes'), each of which defines an area of 400 km^2 (figure 2). A 2-layer (one hidden layer, and one output layer), feed-forward, supervised ANN was utilized in this study. A framework was established (using MATLAB® software) to train 286 separate ANNs (one for each box region) to predict thunderstorm occurrence within each box. NWS forecasters issue public forecasts on the probability of precipitation from thunderstorm activity. However, the highest forecast resolution for the NWS *Zone Forecast* is the county level. The median surface area of the 15 counties in the WFO CRP CWFA is approximately 2256 km^2. Thus an accuracy of 400 km^2 would be a significant improvement. Cloud-to-ground lightning data serves as the proxy for thunderstorm activity and is also the target. The input variables were chosen based on their physical relationship to thunderstorm development/dissipation. For this study, only two boxes are examined – a coastal region near Corpus Christi Texas (box 104), and an inland region near Victoria Texas (box 238). This study is based on data obtained from the period 1 June 2004 through 19 June 2006. Beyond this time period, the NWS replaced the Eta with the non-hydrostatic atmospheric model known as the WRF-NMM (Janjic et. al. 2001). Although the model physics of this model are similar to that of the Eta, model dynamics are different. We prefer not to enhance complexity by requiring the ANN to train from two different atmospheric models.

3.1 Target Data

Cloud to ground (CTG) lightning data was obtained from the National Lightning Detection Network (NLDN) (e.g. Orville 1991). Computer scripts were used to extract hourly lightning data for each of the 286 boxes, and write the output to a series of text files. The MATLAB® software was then used to input the data into a target matrix. This data was used as a proxy for thunderstorm activity. Thus only thunderstorms that generate CTG lightning strikes detected by NLDN are included. The purpose of this ANN is to predict the existence of a thunderstorm within each box. However, instead of creating a target with binary output (lightning versus no lightning), an intermediate condition was included – shower activity. It is hypothesized that training the ANN on both shower and thunderstorm cases would improve the model's ability to predict thunderstorms. Table 1 depicts the criteria used to classify the three scenarios. Showers were identified using the following strategy: (1) Filter out CTG lightning cases. (2) Filter out stratiform rainfall. Hourly rainfall data from a 4-km grid was obtained from a process that integrates data from the Weather Surveillance Radar 88 Doppler (WSR-88D) radars and rain gauges (e.g. Fulton et. al. 1998).

	No Convection	**Shower**	**Thunderstorm**
CTG Lightning	No	No	Yes
R (mm/hr)	≤ 8.0	> 8.0	N/A
Value	0	0.1	1

Table 1: Target Criteria

This data, originally referred to as StageIII, includes hourly rainfall totals. The maximum of the hourly rainfall totals for each box was calculated by Texas A&M University – Corpus Christi (TAMUCC) personnel (see the Acknowledgments section). To filter out stratiform rain cases, a threshold of maximum rainfall rate R >8 mm/hr was used. This rainfall rate threshold value (separating stratiform and convection rainfall) is consistent with those discovered by Morales and Anagnostou (2003) and Grecu et al. (2000).

Figure 3 reveals a 3-D display of the total number of CTG lightning strikes on the 14 x 23 ANN grid (figure 2). Note that the greater number of lightning strikes occurred over the northeast region. This explains one reason for choosing northeast region box 238 – to provide the maximum amount of target data to train this supervised ANN. As will be mentioned later, the limited number of valid lightning cases represented a limitation.

3.2 *Input Data*

The *first* category of data inputs consist of 17 parameters extracted or derived from Eta output. A software program was used to extract the interpolated value of each parameter at the center of each box, which is assumed to be representative of the box. Input to the software are Eta output written to a 12-km Lambert Conformal grid.

CI requires sufficient **moisture** (to generate necessary hydrometeors), atmospheric **instability** (to generate updrafts strong enough to create a charge separation between the liquid and ice phases of water sufficient to generate lightning), and a

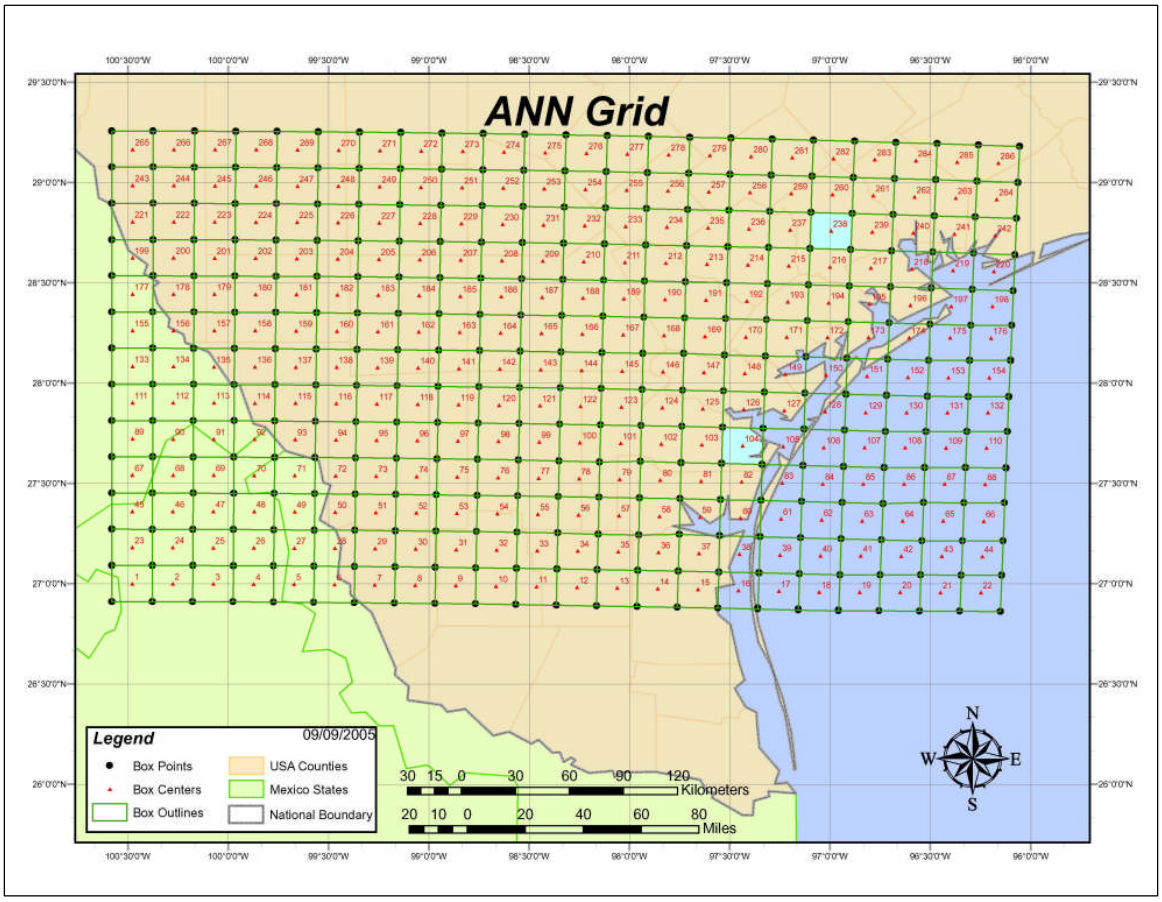

Figure 2: ANN Grid of 14 x 23 equidistant points. Northern (Southern) light blue box is labeled 238 (104).

lifting mechanism (to lift air parcels to the *level of free convection* (LFC), above which an unstable equilibrium exists).

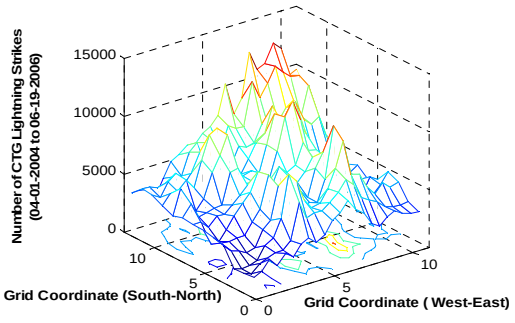

Figure 3: Total CTG Lightning Strikes (6-1-2004 to 6-19-2006) on the ANN grid. Point (0:0) represents the southwest corner (box 1)

The Eta-based output parameters were chosen based on their contribution to the foregoing. As mentioned before, a 12-km grid spacing is insufficient to explicitly forecast convection. However, the purpose of the numerical output is to provide a prediction of those parameters that contribute to CI/convective dissipation in the larger mesoscale environment. The following are the parameters and associated justifications.

***Parameter 1**: Convective precipitation (CP)*

This is the precipitation that represents a byproduct of the CP process. This input is used because an objective of this study is to provide an ANN that will forecast the timing and positioning of convection more accurately than the NWP model. Ideally, the ANN will *learn* to correct CP scheme biases and generate more accurate forecasts.

***Parameters 2-4**: Vertical Velocities at pressure levels 850, 700, and 250 millibars (VV850, VV700, VV250)*

In hydrostatic models, the vertical velocity term is diagnosed from predicted horizontal motions, instead of being predicted explicitly in non-hydrostatic models. VV850 and VV700 are used as proxies for lower level convergence (due to mesoscale phenomena such as sea breezes, and synoptic scale features including fronts) based on the reasoning that the continuity of mass relationship requires upward vertical velocities resulting from surface

convergence. Surface convergence contributes to CI (e.g. Ulanski and Garstang 1978). However, due to its 12-km grid spacing, the Eta cannot resolve the storm scale divergence responsible for the initiation of individual convective cells. The purpose of VV700 and VV250 is to account for upper level disturbances. Operational experience at the NWS National Centers for Environmental Prediction (NCEP) Storm Prediction Center suggests that as many as 50% of thunderstorms are of the elevated variety (Banacos and Schultz, 2005). In these instances, the triggering mechanism is not a surface convergent feature (e.g. surface frontal boundary) but rather mid-level (between 900 and 600 mb) convergence (Wilson and Roberts 2006). The subsequent vertical motions would likely be captured by VV700 and/or VV250. The unstable equilibrium aloft would be captured by the Lifted Index (LI), which will be discussed later.

Parameters 5-8*: U and V components of the wind at 10-m and 850 mb*(u-10, v-10, u-850, v-850)

MODIS-derived high-resolution LST gradients contribute to microscale/meso-γ scale wind patterns that can trigger convection. However, strong wind can minimize the gradients generated by land surface heterogeneity (Dalu et al. 1996; Wang et. al. 1996). The lead author postulates that strong wind will thus preclude thunderstorms that would otherwise be triggered by mesoscale gradients. Thus, it is important to include such wind as input to the ANN model. Further, the lead author has experienced a positive correlation between south/southwest wind at the 850 mb level and atmospheric stability sufficient to preclude CI over deep South Texas. It is hypothesized that such a stable equilibrium condition is caused by the advection of a drier and warmer mid level air mass moving across the region from Mexico.

Parameter 9*: Vertical wind shear between the surface (10-m) and 800 mb* (sh0-8)

Thunderstorm development within a particular 400 km^2 region can be influenced by phenomena in adjacent boxes. However, the ANN in this study does not explicitly account for such. The present ANN model predicts convection for a particular box solely based on information for that box. Including the Eta sh0-8 prediction is one way to account for the influence of conditions over a broader spatial area. Rotunno et. al (1988) suggest that when a gust front (the leading edge of negatively-buoyant air generated by thunderstorms) moves into a environment with a certain shear profile in the lowest 2-km, the subsequent updraft is maximized, which can trigger additional convection. The sh0-8 parameter approximates the 0-2km vertical wind shear. Inputs to the ANN do not include specific information about the gust front. Thus, this parameter is only useful for cases wherein convection within a particular box is generated by gust fronts that enter the box from outside.

Parameter 10*: Vertical wind shear between 800mb and 600 mb (sh8-6)*

Crook (1996) has shown that convection initiation could be prevented by strong vertical wind shear above the planetary boundary layer. The sh8-6 parameter is used as a proxy for the vertical shear encountered by a parcel moving just above the boundary layer.

Parameter 11*: Precipitable water (PW)*

This parameter is the sole moisture input variable. Thunderstorms cannot develop without sufficient atmospheric moisture. Specifically, PW measures the amount of rain that would occur if 100% of atmospheric moisture were to rain out.

Parameter 12*: Lifted Index (LI)*

The Lifted Index (LI) is simply the temperature difference between the environment and an ascending air parcel at the 500mb pressure level. A negative value indicates a parcel warmer than the surrounding environment, thus positively buoyant (unstable equilibrium). As such, it is a measure of atmospheric stability. The primary purpose for inclusion of LI is to account for elevated convection. Elevated convection tends to occur when upper level disturbances move across unstable equilibrium environments aloft. As mentioned before, VV700 and VV250 will serve as proxies for upper level disturbances, and the LI serves as a measure of upper level instability.

Parameters 13-14*: Convective Available Potential Energy (CAPE) and Convective Inhibition (CIN)*

CAPE measures the total energy available to generate thunderstorms. It is computed as the positive area on a thermodynamic diagram (e.g. SkewT-LogP). The greater this value, the greater the energy available for thunderstorm generation. Further, parcel theory indicates that the maximum speed of an updraft is a simple function of CAPE. However, updrafts in nature are generally weaker than what parcel theory suggests owing to turbulent mixing. The CIN measures the negative area on a thermodynamic chart, which typically represents an atmospheric layer starting at the surface. For non-elevated convection to occur, air parcels must be forced from the surface to the top of the CIN layer. However, if CIN is too strong, the parcel cannot reach the LFC and thus CI will not occur.

Parameter 15: *Potential Temperature Drop-off*

Crook (1996) has shown that convection tends to occur over areas wherein the potential temperature (temperature achieved when an air parcel is brought dry adiabatically to 1000 mb) in the boundary layer is lower than the value at the surface. However in this study, the proxy for the boundary layer potential temperature is the potential temperature at 900 mb.

Parameter 16: *Height of the 0^oC Isotherm*

Thunderstorm lightning is thought to occur due to charge separation resulting from the vertical separation of the liquid and solid phases of water, with each containing opposite electrical charge. Thus, this process requires a temperature colder than 0^oC (Saunders 1993). This parameter, when compared to the strength of the updraft (proportional to CAPE based on parcel theory) can be viewed as the extent to which updrafts extend above the

0^{o}C level. Thus, the ANN will have the opportunity to *learn* that lightning is less likely to occur for low CAPE and high 0^{o}C level height.

Parameter 17: *Lifting Condensation Level (LCL)*

Although CAPE measures the total energy available for the conversion to upward vertical velocities, cloud base height (CBH) – according to Williams et. al (2005) – measures the efficiency of this process. A high CBH condition tends to be correlated with an environment that is more efficient than low CBH environments in the conversion to strong updrafts sufficient for thunderstorm development. The LCL is used as a proxy for CBH.

The *second* category of data consists of subgrid scale data to account for processes that are thought to directly trigger convection. The first set of subgrid scale parameters are derived from the MODIS 1-km LST data. Several parameters were computed to serve as proxies for the LST gradient in each box. One such parameter is the *range* (**Parameter 18)** – the difference between the maximum and minimum value of LST. The other LST gradient parameters are the *maximum finite difference* **(Parameters 19 and 20)** between adjacent LST grid point values, in both horizontal orthogonal directions, and the *standard deviation* **(Parameter 21)**. Numerous studies have shown that land surface heterogeneity (resulting in LST gradients) on these scales contribute to the development of micro-α/meso-γ wind fields that contribute to CI (e.g. Avissar and Liu 1996). A significant limitation with regard to MODIS data is the lack of data when clouds exist, which limited a significant number of valid cases. The Daily LST product used was the *LST_Night_1km* SDS (Scientific Data Set) parameter from the *Aqua* (*Terra)* satellite, which moves across the ANN grid generally during the 0645-0825 (0400-0550) UTC period daily. Again, it must be emphasized that the MODIS LST gradients are only measured for *clear-sky* conditions.

The next sub-grid scale input is the *percentage of clear sky* **(Parameter 22)** within each box. CI can occur near/along the location of horizontal thermal gradients generated by a persistent clear-cloudy sky boundary (e.g. Markowski et. al. 1998). It is not uncommon for CI to occur during the afternoon near the location where a clear-cloudy sky boundary occurred earlier in the morning. Although the total percentage of clear sky does not directly correlate to the existence of a cloud boundary, the assumption is that a predominately cloudy or clear sky (i.e. < 10% or > 90%) implies a minimum thermal gradient, whereas percentage values between the extremes indicate a greater likelihood that a cloud edge exists. For each day and box within the analysis time frame, the percentage was calculated from the *LST_Night_1km* SDS parameter from the MODIS *Terra (Aqua)* satellite which provides output for the ANN grid for approximately the 0400-0545 (0645-0825) UTC period daily.

With respect to the LST and clear-sky coverage data, we plan to use more sophisticated data mining techniques (i.e. clustering) in the future to better elucidate the existence of thermal boundaries and gradients within each box.

The *third* sub-grid scale parameter is *Aerosol Optical Depth (AOD)* **(Parameter 23)**, available at 4-km grid spacing (and 15-minute time resolution) from the GOES satellite. Studies suggest that AOD may contribute to the thunderstorm electrification process. In their study of cloud-to-ground lightning over Houston, Texas for the period 1989-2000, Steiger et. al (2002) postulated that increased aerosol concentration may enhance the density of cloud-to-ground lightning strikes. Further, van den Heever et. al. (2005) found that increasing aerosol concentrations can enhance horizontally-averaged convective updraft strength. The AOD data set contains a significant number of missing data. Thus, for each day of the time frame analyzed, data from the 1415, 1515, and 1615 UTC times were used to increase the likelihood of acquiring valid data. This approach is reasonable as Anderson et. al. (2003) have shown that AOD temporal variations at a given location are not significant for time scales $\leq$ 6 hours. Each day, the latest valid data of the three was used to predict CI for the 4-hour period centered at 2100 UTC for the same day (explained in more detail later).

Appendix 1 illustrates the correlation (within box 238) between foregoing parameters 8 (v-850), 10, 11, 13, and 14 (for all days), and the occurrence of CTG lightning (for the 19-23 UTC period each day). The lead author suggests that an ANN will be able to incorporate both the grid-scale numerical model output and sub-grid scale observations and more accurately forecast the timing and position of CI. This hypothesis is based on the reasoning that a model which incorporates both the mesoscale environment conducive to, and microscale processes consistent with, CI should provide optimal solutions and thus more accurate forecasts.

3.3 ANN Training and Testing

The ANN models for this study were developed, trained, and tested within the Matlab® computational environment utilizing the Neural Network Toolbox (The MathWorks, Inc., 2006). All ANN models were trained using the automated regularization algorithm (trainbr) to improve generalization. The ANN architecture for this study is a feed-forward, supervised, multilayer perceptron network with two (2) layers – one hidden layer and an output layer. The transfer function used in both the hidden and output layers is logsig. One hidden neuron was used for this study. The selection of very small ANNs for this model was partly to avoid possible overtraining of the data and based on the success of small [1,1] ANN structures to model the non-linear relationship between winds and predicted water levels (Tissot et al., 2003). Nevertheless, additional hidden neurons did not improve the results. The ANN models were designed to compute each prediction separately resulting in models with one output neuron.

The data sets were divided into one training set and one testing with the even numbered Julian days used for training and odd numbers for testing. The training and testing sets were then alternated resulting in two pairs of training/testing sets. A total of about 750 days were used to be split evenly between the two data sets. After a forecasting time has been set the input and output vectors are created while eliminating cases for which a forecast or

measurement is not available. The ANN model requires a full input set. A screening of the input and target data is performed once the forecast time is selected and cases missing a prediction or measurement are eliminated. After the screening process, approximately 60-80% of the 750 cases were available for training and testing.

In this study, we are testing the ability of the ANN model to forecast CTG lightning occurrence in boxes 104 and 238 for the 4-hour period, centered at 2100 UTC, based on the following inputs:

1: Forecasts from the 12 UTC Eta cycle valid at 2100 UTC.
2: GOES AOD observations at 1415, 1515, or 1615 UTC.
3: MODIS Aqua (Terra) LST gradients from the 0645-0825 (0400-0545) UTC period.
4: MODIS Aqua (Terra) Clear-sky percentage from the 0645-0825 (0400-0545) UTC period

4. RESULTS

ANN model performance was evaluated using the following verification parameters: Probability of Detection (POD), False Alarm Rate (FAR), Critical Success Index (CSI), and the Heidke Skill Score (HSS). Actual lightning observations served as the benchmark. Thus for a given box, POD measures the fraction of cases wherein at least one CTG lightning strike occurred during the 1900-2300 UTC period that was correctly forecast. FAR measures the fraction of ANN forecasts of lightning within a box that did not occur. CSI is the ratio of correct forecasts to the sum of false alarms, misses and correct forecasts. According to the World Meteorological Organization, POD, FAR, and CSI measure **accuracy**, while HSS measures **skill**. Table 2 depicts the verification results for the following eight (8) different combinations of ANN inputs for box 238 (numbers in parentheses are parameter numbers from section 3.2):

Case 1: Eta (1-17)
Case 2: Eta+AOD (1-17; 23)
Case 3: Eta+LST (1-17; 18-21)
Case 4: Eta+Cloud (1-17; 22)
Case 5: Eta+AOD+LST (1-17; 18-21; 23)
Case 6: Eta+AOD+LST+Cloud (1-23)
Case 7: Eta+LST+Cloud (1-17; 18-22)
Case 8: Eta+AOD+Cloud (1-17; 22-23)

The results suggest utility of the ANN model. In this case, the combination of Eta and LST gradient inputs (case 3), and the combination of Eta, LST, and AOD (case 5), resulted in a model that accurately predicted lightning within a 4-hour period centered at 2100 UTC (7-11 hour forecast) greater than 50% of the time (POD=0.58,0.53). However, the false alarm rate was high for each case (FAR=0.84,0.85), resulting in low CSI values. These results suggest that the model is too aggressive in predicting thunderstorm activity. When evaluating based solely on CSI and HSS, the combination of Eta and AOD (case 2) generated the best absolute results (CSI=0.20, HSS=0.25).

Figure 4 depicts the testing of ANN case 3 (even-numbered julian days) for box 238. From this graphical perspective, you can deduce the reason for the high FAR for case 3. However, note that the ANN model performs well given its general tendency to properly forecast thunderstorm occurrence when CTG lightning actually occurred 7-11 hours later.

Case	N	n	POD	FAR	CSI	HSS
1	297	27	0.26	0.74	**0.15**	**0.19**
2	297	27	0.15	0.76	0.10	0.12
3	238	24	0.13	0.77	0.09	0.10
4	249	26	0.19	0.78	0.11	0.12
5	238	24	0.08	0.80	0.06	0.06
6	237	16	**0.44**	0.83	0.14	0.17
7	237	16	0.25	0.80	0.13	0.16
8	249	26	0.19	0.80	0.11	0.10

Table 2a: ANN model verification statistics for testing set: Odd-numbered Julian days. Box 238. 7-11 hour forecast (relative to 1200 UTC Eta cycle) centered at 2100 UTC. The cases refer to the different input combinations tested. N=sample size; n=CTG lightning cases. See text for details.

Case	N	n	POD	FAR	CSI	HSS
1	297	28	0.32	0.71	0.18	0.23
2	297	28	0.36	0.70	**0.20**	**0.25**
3	238	19	**0.58**	0.84	0.15	0.15
4	249	20	0.25	0.77	0.14	0.17
5	238	19	**0.53**	0.85	0.13	0.12
6	238	27	0.22	0.79	0.12	0.12
7	238	27	0.22	0.78	0.13	0.12
8	249	20	0.30	0.70	0.18	0.24

Table 2b: ANN model verification statistics for testing set: Even-numbered Julian days. Box 238. 7-11 hour forecast (relative to 1200 UTC Eta cycle) centered at 2100 UTC. The cases refer to the different input combinations tested. N=sample size; n=CTG lightning cases. See text for details.

The results also indicate the utility of AOD and LST. These parameters appear in two of the three cases that show the most promise in terms of POD, CSI, and HSS. This adds credence to the numerous studies that demonstrate a surface heterogeneity contribution to CI based on LST gradients. With respect to AOD, this study is consistent with the findings of van den Heever et. al. (2005) mentioned earlier.

However, the results for box 104 (not shown) were worse. Yet, we hypothesize that the reason is related to the number of valid lightning cases available to train the model. The number of training cases that included CTG lightning strikes for case 3 was 43 (even+odd numbered Julian days). Yet only around 20 corresponding cases were available for the box 104 case. We speculate that the model will improve as the number of lightning cases increase—As the ANN trains on more lightning events, the better the optimized result.

5. CONCLUSIONS

The hypothesis that an ANN can be developed to improve the forecasting of CI in time and space, by incorporating a combination of mesoscale NWP output (to

incorporate the mesoscale environment) and micro-α/meso-γ scale satellite data (to incorporate expected micro-α/meso-γ convergent flow), was tested.

The results of this study add credence to the foregoing hypothesis. The results indicate that the ANN demonstrates predictability, yet tends to over-forecast events. However,

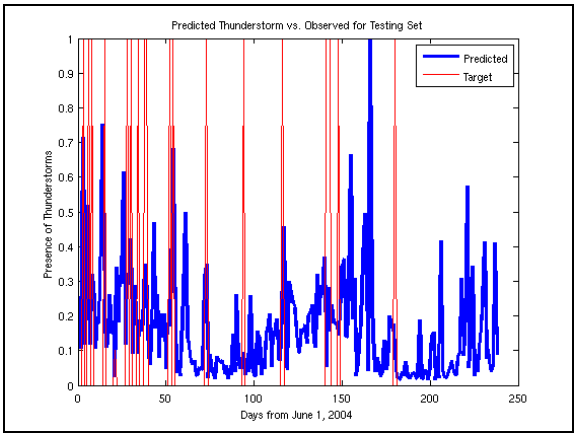

Figure 4: ANN Testing (Case 3; Even-numbered Julian days; Box 238). Any predicted ordinate value (blue-colored lines) of ≥ 0.2 indicates an ANN thunderstorm prediction. The red-colored lines depict CTG lightning observations.

the model's limitation may be related to the amount of lightning data available in this case. Of the 475-594 valid cases available to train the ANN, only 43-55 of them involved lightning strikes. It's probable that this amount of data was insufficient. If so, then the results presented here are not conclusive. Nevertheless, these results suggest that the incorporation of AOD magnitudes and LST gradients enhance the predictability of the ANN model.

We caution that the specific parameters used to elucidate LST gradients (maximum finite differences, range, standard deviation) are likely less than optimal choices. For example, maximum finite differences between adjacent gridpoints do not necessarily indicate that sufficient heterogeneity exists within the box -- necessary to generate the small scale convergent wind patterns thought to trigger convection. We plan to utilize more sophisticated techniques, such as data mining, to better assess whether the necessary thermal gradients and boundaries exist within each box. This is important since the total number of LST data values for each box (400 maximum) can be limited owing to cloud cover, which further complicates the analysis.

Once the data set increases significantly, and more accurate assessments of the thermal gradients that contribute to micro-α and meso-γ convergent flow are conducted, the performance is expected to improve. Further, the authors plan to test whether other AI techniques could improve the results. For example, Genetic Algorithms (Haupt and Haupt, 2004) offer a different approach than the ANN to the optimization problem by incorporating the concept of natural selection.

When evaluating the performance of this ANN in future studies, we plan to incorporate WFO CRP forecaster output as another benchmark. If this ANN performs better than the forecasters in certain cases, it can serve as a supplemental tool when anticipating the timing and position of CI.

Acknowledgments. A number of individuals and organizations provided invaluable assistance. The Federal Aviation Administration (FAA) provided software that the lead author used to calculate the location of the gridpoints that describe the ANN grid. Texas A&M University – Corpus Christi (TAMUCC) student Rick Smith utilized GIS software to confirm that the latitude/longitude values for the ANN domain were calculated correctly. Rick Hay and Russell Carden (TAMUCC) provided the StageIII hourly rainfall data mapped to the ANN boxes. Arthur Taylor (NOAA) provided software to extract the Eta output from Gridded Binary (GRIB) formatted files. Bob Bane provided software for necessary conversions of MODIS output from its native HDF-EOS to NetCDF. Mary Haley and Rick Grubin (UCAR) provided technical assistance with regard to the NCAR Command Language (NCL) used to generate LST gradient output. Ingo Bethke provided software (http://ferret.wrc.noaa.gov/Ferret) to extract the target NLDN data from netCDF-formatted files. Irv Watson (WFO Tallahassee Florida) provided archived NLDN data for the June 2004-October 2005 period. Robert Rozumalski (NOAA) provided Eta output for the January-October 2005 period. Dan Swank (NCDC/NOMADS) provided the Eta output for the June-December 2004 period. Brett Lien, Carolyn Gacke, Calli Jenkerson (NASA/LP DAAC), and Zhengming Wan (University of California – Santa Barbara) provided technical assistance with regard to the MODIS data. Chuanyu Xu and Shobha Kondragunta (NOAA/NESDIS) provided GOES AOD data, and Jun Wang (Harvard University) provided useful knowledge regarding the various AOD data sources. The lead author received a U.S. Department of Commerce Pioneer Grant to purchase the necessary computer hardware, and the MATLAB® software, for this study. With respect to the generation of this manuscript, Natalia Nolazco provided invaluable formatting and graphical assistance.

References

Anderson, T. L., R. J. Charlson, D. M. Winker, J. A. Ogren, K. Holmén, 2003: Mesoscale Variations of Tropospheric Aerosols. *J. Atmos. Sci*. **60**, 119-136.

Avissar, R., and Y. Liu. 1996. Three-dimensional numerical study of shallow convective clouds and precipitation induced by land surface forcing. *J. Geophys. Res.* **101**, 7499-7518.

Banacos, P. C., and D. M. Schultz. 2005. The Use of Moisture Flux Convergence in Forecasting Convective Initiation: Historical and Operational Perspectives. *Wea. Forecasting*. **20**, 351-366.

Beale, R. 1990. *Neural Computing: An Introduction*. Institute of Physics Publishing, London.

Crook, N. A. 1996. Sensitivity of Moist Convection Forced by Boundary Layer Processes to Low-Level Thermodynamic Fields. *Mon. Wea. Rev.* **124**, 1767-1785.

CyRDAS, 2004. Cyberinfrastructure for the Atmospheric

Sciences in the 21st Century. Boulder, CO: National Center for Atmospheric Research (NCAR); Ad Hoc Committee for Cyberinfrastructure Research, Development and Education in the Atmospheric Sciences (CyRDAS), 56 p.

Dalu, G. A., R. A. Pielke, M. Baldi, X. Zeng. 1996: Heat and Momentum Fluxes Induced by Thermal Inhomogeneities with and without Large-Scale Flow. *J. Atmos. Sci*. **53**, 3286-3302.

Fabry, F. 2006. The Spatial Variability of Moisture in the Boundary Layer and Its Effect on Convective Initiation: Project-Long Characterization. *Mon. Wea. Rev.* **134**, 79-91.

Fulton, R. A., J. P. Breidenbach, D-J Seo, T. O'Bannon, and D. A. Miller, 1998: The WSR-88D Rainfall Algorithm. *Wea. Forecasting*, **13**, 377-395.

Grecu, M., E. N. Anagnostou, and R. F. Adler, 2000: Assessment of the Use of Lightning Information in Satellite Infrared Rainfall Estimated. *Journal of Hydrometeorology*. **1**, 211-221.

Hagan, M. T., H. B. Demuth, and M. Beale, 1996: Neural Network Design, International Thomson Publishing Inc.

Haupt, R. L., and S. E. Haupt, 2004: Practical Genetic Algorithms, John Wiley and Sons.

Janjic ZI, Gerrity JP, Nickovic S (2001) An Alternative Approach to Nonhydrostatic Modeling. Monthly Weather Review: Vol. **129**, No. 5 pp. 1164–1178

Kalnay E., 2003: Atmospheric Modeling, Data Assimilation and Predictability. Cambridge University Press, Cambridge, United Kingdom.

Markowski, P. M., E. N. Rasmussen, J. M. Straka, and D. C. Dowell, 1998: Observations of low-level baroclinicity generated by anvil shadows. *Mon Wea. Rev.*, **126,** 2942–2958.

Mass, C. F., D. Owens, K. Westrick, B. A. Colle, 2002: Does Increasing Horizontal Resolution Produce More Skillful Forecasts? *Bull. Amer. Meteor. Soc.*, 407-430.

Morales, C., and E. N. Anagnostou, 2003: Extending the Capabilities of Rainfall Estimation from Satellite Infrared via a Long-Range Lightning Network Observations. *Journal of Hydrometeorology* 4(2), 141-159.

Orlanski, 1975: A Rational Subdivision of Scales for Atmospheric Processes. Bull. Amer. Meteor. Soc., **56**, 527-530.

Orville, R. E., 1991: Lightning ground flash density in the contiguous United States—1989. *Mon. Wea. Rev.*, **119,** 573–577

Pielke, R. A., 2002: *Mesoscale Meteorological Modeling*. International Geophysics Series, Vol. 78. Academic Press, San Diego. 676pp.

Rogers, E., T. L. Black, D. G. Deaven, and G. J. DiMego, 1996: Changes to the operational "early" Eta analysis/forecast system at the National Centers for Environmental Prediction. *Wea. Forecasting*, **11,** 391–413.

Rotunno, R., J. B. Klemp, and M. L. Weisman. 1988. A Theory for Strong, Long-Lived Squall Lines. *J. Atmos. Sci*. **45**, 464-485.

Saunders, C. P. R., 1993: A Review of Thunderstorm Electrification Processes. *J. Appl. Meteor*. **32**, 642-655.

Steiger, S. M., R. E. Orville, and G. Huffines, 2002: Cloud-to-ground lightning characteristics over Houston, Texas: 1989-2000. *Journal of Geophysical Resarch*, 107, No. D11, 10.1029/2001JD001142

P.E. Tissot, D.T. Cox, and P.R. Michaud, 2003: "Optimization and Performance of a Neural Network Model Forecasting Water Levels for the Corpus Christi, Texas, Estuary", 3rd Conference on the Applications of Artificial Intelligence to Environmental Science, Long Beach, CA, Amer. Meteor. Soc.

Ulanski, S. L., and M. Garstang. 1978. The role of surface divergence and vorticity in the life cycle of convective rainfall. Part I. Observations and analysis. *J. Atmos. Sci*. **35,** 1047-1062.

Van den Heever, S.C., G. G. Carrió, W. R. Cotton, and W. C. Straka, 2005: The impacts of Saharan dust on Florida storm characteristics. Preprints, *16th Conference on Planned and Inadvertent Weather Modification*, San Diego, CA, Amer. Meteor. Soc.

Wang, J., R. L. Bras, and E. A. B. Eltahir. 1996. A Stochastic Linear Theory of Mesoscale Circulation Induced by Thermal Heterogeneity of the Land Surface. *J. Atmos. Sci*. **53**, 3349-3366.

Williams, E. R., V. Mushtak, D. Rosenfeld, S. Goodman, and D. Boccippio. 2005. Thermodynamic conditions favorable to superlative thunderstorm updraft, mixed phase microphysics and lightning flash rate. *Atmos. Res*., **76**, 288-306.

Wilson, J. W., and R. D. Roberts. 2006. Summary of Convective Storm Initiation and Evolution during IHOP: Observational and Modeling Perspective. *Mon. Wea. Rev*., **134**, 23-47.

Zeng X., and R. A. Pielke. 1995. Further Study on the Predictability of Landscape-Induced Atmospheric Flow. *J. Atmos. Sci. **52**, 1680-1698*

Appendix 1: Graphic Comparison of Lightning Occurrences with Selected Eta Predicted Parameters